IET Image Processing

Special Section: Multidisciplinary advancement of imaging technologies: from medical diagnostics and genomics to cognitive machine vision, and artificial intelligence

IET Journals
The Institution of Engineering and Technology

Evaluation of nano-filler dispersion quality in polymeric films with binary feature characteristics and fractal analysis

ISSN 1751-9659
Received on 12th November 2019
Revised 22nd May 2020
Accepted on 1st June 2020
E-First on 6th July 2020
doi: 10.1049/iet-ipr.2019.1512
www.ietdl.org

Kazim Yildiz[1] ✉, *Zehra Yildiz*[2]

[1]*Department of Computer Engineering, Faculty of Technology, Marmara University, Istanbul, Turkey*
[2]*Department of Textile Engineering, Faculty of Technology, Marmara University, Istanbul, Turkey*
✉ *E-mail: kazim.yildiz@marmara.edu.tr*

Abstract: This study investigates the use of binary features and fractal dimension analysis to evaluate the dispersion quality of nanofillers in thin polymeric films by using light microscopy images. For this purpose, polymeric films were cast with the inclusion of various montmorillonite (MMT) nanofiller amounts. Then the light microscopy images were captured from the polymeric films then preprocessed for the evaluation. Thresholding process was applied to the obtained images for each nanofiller percentage level. The obtained binary level images were used in the feature extraction process with binary statistics and fractal dimension. Thermogravimetric analysis (TGA) was used to evaluate the flame resist behaviour of polymeric films based on the dispersion quality of nanofillers. The samples with various nanofiller contents were tested using the image processing method and the results were all compared with the TGA results. The results obtained by the feature extraction process and TGA, about the dispersion quality of nanofillers, were all in good agreement.

1 Introduction

Characterisation of the nanofiller dispersion quality of polymeric films is very important considering the materials' quality-related properties such as thermal, chemical, mechanical, comfort etc. The nanofiller amount and dispersion quality can be analysed by various experimental processes to show the inner structure in detailed. The dispersion quality of nanofillers in polymeric films determines the suitability of films for many applications such as coating, varnishes, and other usage areas, and gives information about the performance of the end product.

Microscopic image of a composite material demonstrates visible morphological properties related to the inner structure such as clusters, dispersion and agglomeration. These properties generally give an idea about the dispersion quality of the fillers. Through proper analysis of microscopic images, the dispersion quality can be quantified with the help of morphological structures. In such kind of works, scanning electron microscopy (SEM) images are used to get information about the inner structure of materials. If the microscopic images are effectively characterised, it is easy to define the dispersion quality of the fillers in composites for different particle contents. The characterisation of the inner structure of composites by using the image processing techniques has been intensively searched recently. For instance, the digital image processing technique has been proposed to define the relationship between crack shapes and wearing loss by using SEM images [1]. Texture feature extraction and classification methods have been used for wheat straw/polypropylene composites in order to accelerate the aging test [2]. In another research, the SEM images have been used in an image processing technique to estimate the filler content of polymeric nanocomposites [3]. For anodic porous alumina, structural characterisation analysis has been introduced with SEM images [4] and fractal dimension calculation has been used for identification the polymeric nanocomposites [5]. Tanaka *et al.* [6] have extracted various physical information about the polymeric composites from the optical microscope images of the composite. Grassini *et al.* [7] have proposed a wavelet image decomposition for characterisation of freeze-dried pharmaceutical product structures. Bhatia *et al.* [8] have used image processing to measure the drop profile coordinates and their distribution for different surfaces. Lampasi *et al.* [9] have proposed the morphological and functional characterisation of nanostructured thin polymeric films. Sasov *et al.* [10] have searched about the one- and two-dimensional Fourier transform for quantitative analysis of polymeric structures. Image processing tools have also been used to quantitatively assess the granulometry of the catalyst and polymer granules in polymer blends [11–13]. Song *et al.* [14] have determined the grey threshold algorithm to compare and analyse the results with vacuum water saturating method and nuclear magnetic resonance for pore structure characterisation and permeability. Campbell *et al.* [15] have proposed a new set of automated techniques for 2D microstructural analysis. The proposed techniques have the capability on a variety of microstructure types and both SEM and microscopy images. Meng *et al.* [16] have proposed an image analysis method of particle size distribution with modified canny edge detection and Hough transform. Experimental results have shown that the proposed method recognise the particles with high accuracy. Yildiz [17] has suggested a method for an objective and a cost-effective method in order to separate wool fibre from mohair fibre by using the identification method. The obtained results have effective on microscopic images to classify with the deep learning method. In another study, geometric substances in irregular shapes have been studied with the fractal dimension, which can reflect the characteristic is appearing in nature. It has been used to explain numerous fragmenting and branching in various fields. The output has a binarised image with a one-pixel-wide boundary appropriate to be used for box-counting calculations for the approximate fractal dimension of the boundary. The box-counting technique has been implemented for fractal dimension calculations [18–20].

Agglomeration of the solid particles refers to the non-uniform dispersion of the particles in film/composite structure. The agglomerated areas in a polymeric thin film can be seen easily with the naked eye or via microscopic techniques. The agglomeration level defines the dispersion level of the particles that are related to the quality of the polymeric film. The material scientists quantify the dispersion level with the help of SEM or light microscopy images. Then the obtained images can be used in image processing techniques in order to compare some experimental results such as flame retardancy test, thermogravimetric analysis (TGA), antibacterial activity etc. This study can be accepted as a novel since the usage of image processing technique for determination of

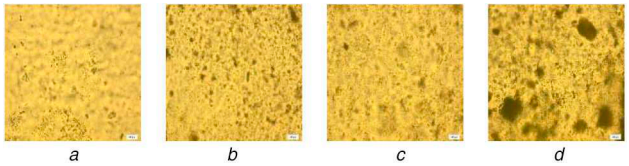

Fig. 1 *Light microscopy images of UV-cured polymeric films in various MMT amounts*
(a) 1%, ***(b)*** 3%, ***(c)*** 5%, ***(d)*** 7%

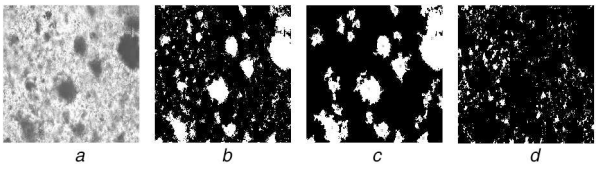

Fig. 2 *Example of*
(a) Original grey level image, ***(b)*** Binary image, ***(c)*** Agglomerated objects detection, ***(d)*** Removing the agglomerated areas from the image

dispersion quality levels of nanoparticles in polymeric films for the comparison of TGA results, has never been tried before. In this study, the light microscopy images of the polymeric films containing MMT nanoclay particles were used to compare the TGA results of these films with the help of the dispersion level of the solid particles. First, the polymeric films were casted in three different MMT percentages then the microscopic images were captured from the film surfaces. In the preprocessing stage, the images were processed for feature extraction. The fractal and morphological analyses were generated for feature extraction. According to the feature matrix, the microscopic images were recognised and classified with Naïve Bayesian. The image analysis can provide a new characterisation and evaluation aspect regarding the dispersion quality of solid particles inside the polymeric films. Comparing the results of TGA and image processing, this study gives promising results to define the dispersion quality.

2 Experimental setup

2.1 Preparation of polymeric films

Polymeric films were produced with the TDI-HEMA-PVB synthesis reaction as in previous studies [21, 22]. A round-bottom flask equipped with a magnetic stirrer, a nitrogen gas inlet and a condenser were used for the reaction medium. TMPTMA (50 wt.%) was used as a reactive diluent. The synthesis reaction was performed at 3 h at 75°C. Polymeric films were then cast by using photoinitiator and MMT nanoclay as nanofiller in various percentages (1, 3, 5, 7 wt.%) then exposed to UV-light for 4 min between two glass plates. Before casting the films, a magnetic stirrer was used to disperse the clay particles homogeneously in the solution. The light microscopy images of polymeric films were captured by using an Olympus BX51 microscope (Fig. 1). Thirty different images with the size of 2080 × 1544 pixels were captured from the polymeric film surface for each MMT percentage. Then the obtained images were used in the image processing technique.

2.2 Thermal gravimetric analysis

MMT is a type of inorganic, economical, recyclable, non-toxic clay, which is typically consisting of one octahedral aluminate layer that is sandwiched between two octahedral silicate layers. It has intrinsically flame retardant property. In the literature, several studies have been made investigating the flame resist behaviour of MMT in composites [23, 24]. TGA is used to investigate the physical, chemical properties and thermal decomposition character of material as a function of increasing temperature. By using TGA, flame resist behaviour of composites can be searched. In this study, TGA (TA TGA Q50 instrument, under nitrogen flow, with a heating rate of 10°C/min, between 30 and 600°C) was employed to observe the flame resist properties of the prepared polymeric films with various MMT amounts.

2.3 Thresholding and binarisation

The light microscopy images of polymeric films were converted to binary level to represent the polymer and filler zones. In order to identify the percentage of filler content, an appropriate threshold value was chosen. Through visual investigation of binary images, the MMT fillers in microscopic images are shown in white colour. After thresholding, the agglomerated particles were removed from binary image with a predefined threshold level that was set during the polymeric film casting process. In order to remove the agglomerated areas from the image (Fig. 2*c*), the image was masked with thresholder thus a uniform dispersion image was obtained without any agglomerated area (Fig. 2*d*). This process can be seen in Fig. 2. During the thresholding and binarisation processes, various surface characteristics such as the total area, the number of objects, average distance between objects, number of agglomerated objects, the total area of agglomerated objects, the average area of agglomerated objects, irregularity and standard deviation of agglomerated objects were all used as features in order to define the MMT percentages. In the binary level, eight different features and fractal dimension were used for the evaluation process.

The object area and the total area were calculated for all the particles. All distances between each object pairs were calculated. The average value of the distance was used as a feature. In order to calculate the pairwise distance, Euclidean distance metric was used. The Euclidean distance between pairs can be defined according to the following equation:

$$d_{\mathrm{st}}^2 = (\boldsymbol{x}_{\mathrm{s}} - \boldsymbol{y}_{\mathrm{t}})(\boldsymbol{x}_{\mathrm{s}} - \boldsymbol{y}_{\mathrm{t}})^{\mathrm{I}} \quad (1)$$

where $\boldsymbol{x}_{\mathrm{s}}$ and $\boldsymbol{y}_t$are given as vectors, which are objects centroids. These centroid values are used to define the Euclidean distance between pair objects. Then, the average value of the distance is used for the feature.

2.4 Fractal dimension and image analysis

The word fractal means that it is a kind of figure that consists of similar small elements in irregular shapes. It can be accepted as an alternative to the Euclidean geometry for the identification of natural structures. Fractal dimension quantifies the features of objects or characteristics of the event, which are shape, texture, number, colour, repetition, similarity, randomness, regularity and heterogeneity [25]. Thus, the fractal dimension can be explained as a feature tool used to interpret several texture features [26–28].

The most common method of calculating the fractal dimension is the box-counting method. In this method, the shape or image of a particular size is coated with box. For different sizes of boxes counted the number of the box with the shape of a part at a time and log-log scale to the number of the squares is applied with a full box. According to Fig. 3, boxes laid over an image of a sample with a certain size. The boxes are situated with a repeated position through the image.

Fractal dimension is defined as the slope obtained from (2). Box counting method, is concerned with self-affinity size and gives the same number in most cases. The following equation shows the relation between the scale factor r and box number $N(r)$;

$$D_f = \frac{\log(N(r))}{\log\left(\frac{1}{r}\right)} \tag{2}$$

According to (2), an image can be divided by r and $N(r)$ that are run on the same property. The r is reduced while the process is continued. In the process, the number of boxes is determined for each value of r. According to the $N(r)$ of r is plotted. The slope of D_f, which is obtained from (2), is related to the image without any agglomerated area (Fig. 2*d*) [29]. In this study, after finding the slope from (2), the mean values for each binary images were used as a feature to define the dispersion quality of polymeric composites with other binary features. Additionally, the value of the fractal dimension was found as 1.9 on an average.

2.5 Classification by Naïve Bayes

Naïve Bayes classifier networks are the basic model among Bayesian networks. Friedman *et al.* [30] describe the term of 'Naïve' as the strong independence hypothesis between variables. A class node is the main element of all attribute nodes, which are graphically represented by a hierarchical structure [30, 31]. Therefore, the Naïve Bayes is the possibility of a given sample that is belonging to a certain class node [32]. All attributes are represented by each node. For each value of the relevant attribute, it is related to the conditional probability table (CPT), which contains all the conditional probabilities according to the values of the class nodes [33]. In this study, the Naïve Bayes algorithm was used to classify the coating quality of polymeric composites by using the fractal dimension and binary features.

3 Results and discussion

The light microscopy images of the samples in four different MMT contents were given in Fig. 1. For each MMT amount, 30 different images were captured. It can be seen that a well-dispersed and homogeneous coating layers were obtained in Figs. 1*a*–*c*, whilst in Fig. 1*d*, some agglomeration of nanoparticles in the coating layer were observed as black regions. It was assumed that 5% nanoparticle inclusion to the coating layer could be accepted as optimum concentration. After that, in 7% nanoparticle inclusion, agglomeration occurs due to the particle holding capability of fabric in its pores. This result is also consistent with the TGA results, as can be seen in Table 1. Accordingly, the increment in nanofiller content caused an increase in char yield. In other words, MMT inclusion to the formulation increases the flame resist behaviour to 5%. Although 7% of nanofiller inclusion has the highest nanofiller content, the highest char residue in other words, the best flame resist behaviour was observed in 5% nanofiller inclusion.

In this paper, based on the flame retardant property, the coating quality levels were defined as best, good, average, and poor for each MMT loadings. Fig. 4 shows the score plot of the number of agglomerated objects for each quality level based on 60 test samples 15 for each level. It is possible to see that all quality levels of the composites were separated distinctly from each other. Although only a few samples' coating quality levels were recorded as 'average', the number of samples in 'best' and 'good' quality levels were so close to each other. So it is clear that the coating quality levels can be identified easily by using these features; average distance between all objects, number of objects, the average area of objects, fractal dimension, and number of agglomerated areas. Among all these features, the number of the agglomerated area has a very excellent ability for characterisation and discrimination of the microscopy images of the polymeric films in different particle loadings. The best quality level belongs to the sample containing 5% MMT. This result is also consistent with the TGA result. According to Fig. 4, although the average quality level has the lowest agglomerated area, it cannot be accepted as best level due to having a very little amount of MMT as can be seen in Fig. 1*a*.

Table 2 shows the classification results as a confusion matrix. In the classification process, four features were used; average distance between all objects, number of objects, the average area of objects, and fractal dimension. As can be seen in Table 2, 15 test and train images for each quality level, so totally 60 test and train images, were all used in the confusion matrix. According to the results, the 'best' coating quality level was recorded with a 100% accuracy rate. In the 'poor' coating quality level, only one sample was classified as 'best'. For 'good' and 'average' coating quality levels,

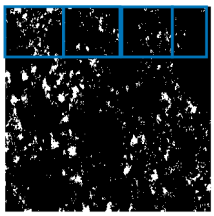

Fig. 3 *Example of boxes on an image*

Table 1 Thermogravimetric data of the UV-cured polymeric films

Montmorillonite amount, %	Char yield, %	Quality levels
1	9.1	average
3	10.7	good
5	12.6	best
7	8.8	poor

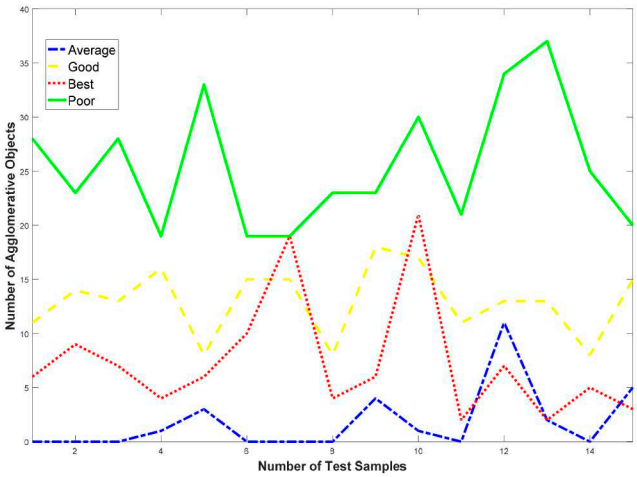

Fig. 4 *Quality levels in terms of the number of agglomerated area for fifteen test samples per level*

Table 2 Classification results and accuracy rates as a confusion matrix with four features

	Best	Good	Average	Poor	Classification accuracy, %
best	15	0	0	0	100
good	0	13	0	2	86.7
average	2	0	13	0	86.7
poor	1	0	0	14	93.3
overall classification accuracy, %					91.7

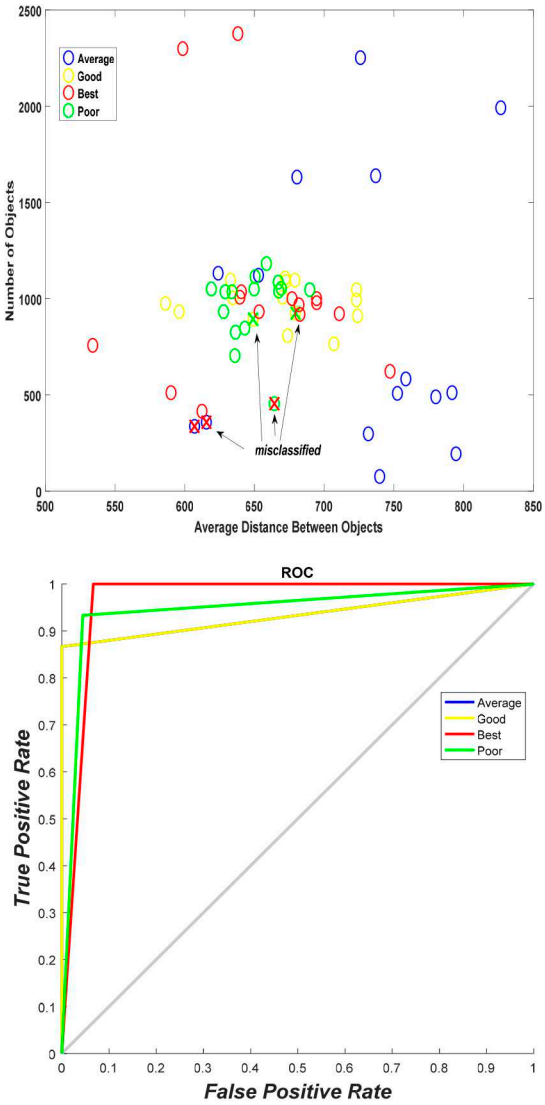

Fig. 5 *Classification results of microscopy image of samples in four different coating levels with its ROC curves by using four features*

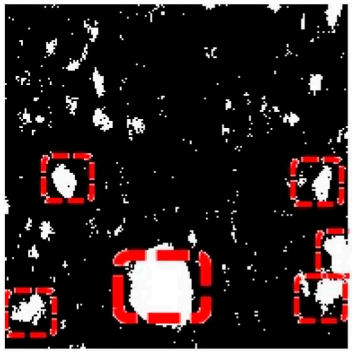

Fig. 6 *Binary image of 7% MMT included coating to show the agglomerated areas on the coating surface*

two samples from both of them were classified wrongly. The overall classification accuracy for the experiment was found as 91.7%. The classification scheme with a number of objects and the average distance between objects features and its receiver operating characteristic (ROC) curve were all illustrated in Fig. 5.

In the experimental process, the agglomerated areas were evaluated by using the mentioned four features. Agglomeration means an irregular allocation of nanofillers resulting in non-uniform dispersion. Thus, fillers stick together and appear in greater dimensions than they really are. Fig. 6 shows the agglomerated areas in red squares that belong to 7% MMT included coating. The agglomerated areas were counted and extracted as a feature for adding feature vector in order to make a decision about the size of the agglomerated area. After the binarisation process, small objects were selected on the surface and removed. Then the rest of the image was subtracted from the original one to find the bigger ones; in other words, the agglomerated areas.

After adding the number of agglomerated areas into the feature vector, the classification result can be seen in Table 3. Best, good and average coating quality levels were classified truly. Only one level from poor coating was misclassified. So the total

Table 3 Classification results and accuracy rates as a confusion matrix with five features

	Best	Good	Average	Poor	Classification accuracy, %
best	15	0	0	0	100
good	0	15	0	0	100
average	0	0	15	0	100
poor	0	1	0	14	93.3
overall classification accuracy, %					98.3

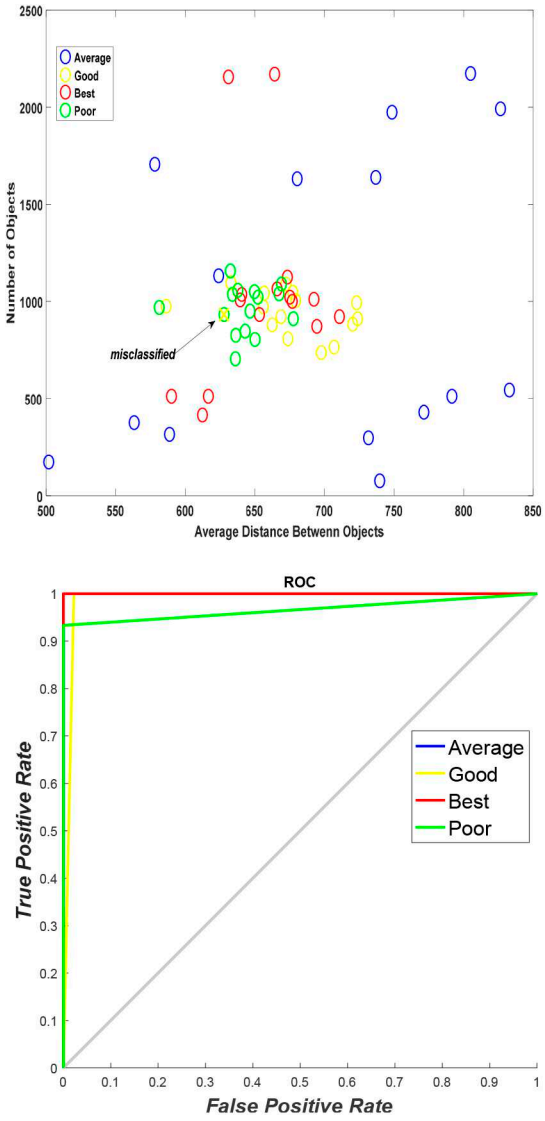

Fig. 7 *Classification results of microscopy image of samples in four different coating levels with its ROC curves by using five features*

Table 4 Classification results and accuracy rates as a confusion matrix with nine features

	Best	Good	Average	Poor	Classification accuracy, %
best	15	0	0	0	100
good	0	15	0	0	100
average	0	0	15	0	100
poor	0	0	0	15	100
overall classification accuracy, %					100

classification accuracy was found as 98.3%. The feature of the number of agglomerated areas helped to determine the different MMT percentages in coatings. Thus, classification performance was affected positively. Fig. 7 shows the classification schema of the number of objects and the average distance between objects features with its ROC curve by using five features.

In the previous experiment, five features were used for the feature extraction process while at this time, another four features were added to enhance the classification accuracy. These are a total area of agglomerated objects, the average area of agglomerated objects, irregularity, and standard deviation. Table 4 gives the classification results of agglomerated images by using nine features. Fig. 8 shows the classification schema of the number of objects and the average distance between objects features with its ROC curve by using nine features. Accordingly, the best classification accuracy with 100% was obtained with the usage of nine features. It can be seen that whenever the number of feature

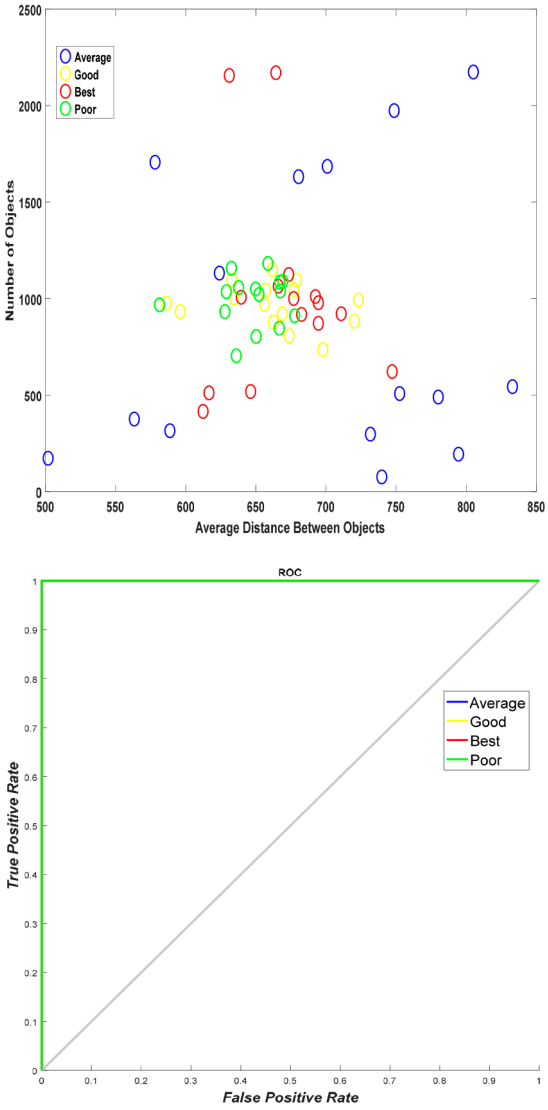

Fig. 8 *Classification results of microscopy image of samples in four different coating levels with its ROC curves by using nine features*

vectors increases, the classification accuracy also increases. So all samples were classified correctly when nine features were used.

4 Conclusion

The aim of this study was to develop a quality classification method for particle added polymeric films by using an image processing technique. For this purpose, polymeric films were cast with the inclusion of nanoparticles (MMT) in various percentages and then evaluated in terms of the flame retardant property by using TGA. According to the TGA results, the highest flame retardant property was recorded in 5% MMT included a sample. Then the light microscopy images of these polymeric films were captured and used in order to obtain the binary features and fractal dimensions during the feature extraction process. Results proved that the binary feature characteristic and fractal dimension method could both well describe the textural feature of the microscopic images of polymeric films with particle loaded in various percentages. The binary feature characteristics such as the average distance between objects, total filler area, number of fillers, and the number of agglomerated objects were all showed effective and feasible results for evaluation of nanofiller dispersion quality in polymeric films. Naïve Bayesian classifier was applied on the light microscopy images of polymeric films in four different coating quality levels for identification. The best classification accuracy was recorded by using nine discriminative features. The classification process of microscope images was performed by using the fractal dimension and binary features, and verified based upon TGA results, successfully. Future work will be in the way of classification the coating quality levels depending on the quantitative characterisation of polymeric composites.

5 References

[1] Zhou, Y., Pervin, F., Jeelani, S., *et al.*: 'Improvement in mechanical properties of carbon fabric–epoxy composite using carbon nanofibers', *J. Mater. Process. Technol.*, 2008, **198**, (1), pp. 445–453

[2] Zhang, H., He, C., Yu, M., *et al.*: 'Texture feature extraction and classification of SEM images of wheat straw/polypropylene composites in accelerated aging test', *Adv. Mater. Sci. Eng.*, 2015, **2015**, Article ID 397845, https://doi.org/10.1155/2015/397845

[3] Kundu, S., Jana, P., De, D., *et al.*: 'SEM image processing of polymer nanocomposites to estimate filler content'. 2015 IEEE Int. Conf. on Electrical, Computer and Communication Technologies (ICECCT), Coimbatore, India, 2015

[4] Raimundo, D.S., Calíope, P.B., Huanca, D.R., *et al.*: 'Anodic porous alumina structural characteristics study based on SEM image processing and analysis', *Microelectron. J.*, 2009, **40**, (4), pp. 844–847

[5] Lashgari, A., Ghamami, S., Shahbazkhany, S., *et al.*: 'Fractal dimension calculation of a manganese-chromium bimetallic nanocomposite using image processing', *J. Nanomater.*, 2015, **2015**, p. 144

[6] Tanaka, H., Hayashi, T., Nishi, T.: 'Application of digital image analysis to pattern formation in polymer systems', *J. Appl. Phys.*, 1986, **59**, (11), pp. 3627–3643

[7] Grassini, S., Angelini, E., Pisano, R., *et al.*: 'Wavelet image decomposition for characterization of freeze-dried pharmaceutical product structures'. 2015 IEEE Int. Instrumentation and Measurement Technology Conf. (I2MTC), Pisa, Italy, 2015

[8] Bhatia, Q.S., Chen, J.-K., Koberstein, J.T., *et al.*: 'The measurement of polymer surface tension by drop image processing: application to PDMS and comparison with theory', *J. Colloid Interface Sci.*, 1985, **106**, (2), pp. 353–359

[9] Lampasi, D.A., Tamburrano, A., Bellini, S., *et al.*: 'Effect of grain size and distribution on the shielding effectiveness of transparent conducting thin films', *IEEE Trans. Electromagn. Compat.*, 2014, **56**, (2), pp. 352–359

[10] Sasov, A.Y., Ermakova, T., Lotmentsev, Y.M.: 'Quantitative analysis of images depicting structure of polymers and polymer composites', *Polymer Sci. USSR*, 1991, **33**, (3), pp. 597–602

[11] Bailly, J., Hagege, R.: 'Use of image analysis for the knowledge and control of polymer and Ziegler-Natta catalyst granulometry', *Polymer*, 1991, **32**, (1), pp. 181–190

[12] Jose, A.J., Wong, L.S., Merrington, J., *et al.*: 'Automated image analysis of polymer beads and size distribution', *Ind. Eng. Chem. Res.*, 2005, **44**, (23), pp. 8659–8662

[13] Harrats, C., Blacher, S., Fayt, R., *et al.*: 'Molecular design of multicomponent polymer systems XIX: stability of cocontinuous phase morphologies in low-density polyethylene–polystyrene blends emulsified by block copolymers', *J. Polym. Sci., Part B: Polym. Phys.*, 1995, **33**, (5), pp. 801–811

[14] Song, S.-B., Liu, J.-F., Yang, D.-S., *et al.*: 'Pore structure characterization and permeability prediction of coal samples based on SEM images', *J. Nat. Gas. Sci. Eng.*, 2019, **67**, pp. 160–171

[15] Campbell, A., Murray, P., Yakushina, E., *et al.*: 'New methods for automatic quantification of microstructural features using digital image processing', *Mater. Des.*, 2018, **141**, pp. 395–406

[16] Meng, Y., Zhang, Z., Yin, H., *et al.*: 'Automatic detection of particle size distribution by image analysis based on local adaptive canny edge detection and modified circular Hough transform', *Micron*, 2018, **106**, pp. 34–41

[17] Yildiz, K.: 'Identification of wool and mohair fibres with texture feature extraction and deep learning', *IET Image Process.*, 2020, **14**, pp. 348–353

[18] Burrough, P.: 'Fractal dimensions of landscapes and other environmental data', *Nature*, 1981, **294**, (5838), pp. 240–242

[19] Milne, B.T.: 'Measuring the fractal geometry of landscapes', *Appl. Math. Comput.*, 1988, **27**, (1), pp. 67–79

[20] Du, C.-J., Sun, D.-W.: 'Recent developments in the applications of image processing techniques for food quality evaluation', *Trends Food Sci. Technol.*, 2004, **15**, (5), pp. 230–249

[21] Yildiz, Z., Onen, H.A.: 'Dual-curable PVB based adhesive formulations for cord/rubber composites: the influence of reactive diluents', *Int. J. Adhesion Adhes.*, 2017, **78**, pp. 38–44

[22] Yildiz, Z., Aysen Onen, H., Gungor, A., *et al.*: 'Synthesis and application of dual-curable PVB based adhesive formulations for cord/rubber applications', *J. Adhes. Sci. Technol.*, 2017, **31**, (17), pp. 1900–1911

[23] White, L.A.: 'Preparation and thermal analysis of cotton–clay nanocomposites', *J. Appl. Polym. Sci.*, 2004, **92**, (4), pp. 2125–2131

[24] Apaydin, K., Laachachi, A., Ball, V., *et al.*: 'Polyallylamine–montmorillonite as super flame retardant coating assemblies by layer-by layer deposition on polyamide', *Polym. Degrad. Stab.*, 2013, **98**, (2), pp. 627–634

[25] Herbert, J., Cameron, J., Matthew, W.: 'Is there meaning in fractal analysis', *Complexity Int.*, 1999, **6**, pp. 144–149

[26] Xian, Y., Liu, J., Zhang, C., *et al.*: 'Fractal characteristics of fracture morphology of steels irradiated with high-energy ions', *J. Nucl. Mater.*, 2015, **461**, pp. 171–177

[27] Hilders, O.A., Ramos, M., Peña, N.D., *et al.*: 'Fractal geometry of fracture surfaces of a duplex stainless steel', *J. Mater. Sci.*, 2006, **41**, (17), pp. 5739–5742

[28] Wickens, D., Lynch, S., West, G., *et al.*: 'Quantifying the pattern of microbial cell dispersion, density and clustering on surfaces of differing chemistries and

topographies using multifractal analysis', *J. Microbiol. Methods*, 2014, **104**, pp. 101–108
[29] Foroutan-Pour, K., Dutilleul, P., Smith, D.: 'Advances in the implementation of the box-counting method of fractal dimension estimation', *Appl. Math. Comput.*, 1999, **105**, (2), pp. 195–210
[30] Friedman, N., Geiger, D., Goldszmidt, M.: 'Bayesian network classifiers', *Mach. Learn.*, 1997, **29**, (2–3), pp. 131–163
[31] Duda, R.O., Hart, P.E., Stork, D.G.: '*Pattern classification*' (John Wiley & Sons, New York, USA, 2012)
[32] Cooper, G.F., Herskovits, E.: 'A Bayesian method for the induction of probabilistic networks from data', *Mach. Learn.*, 1992, **9**, (4), pp. 309–347
[33] Feki-Sahnoun, W., Njah, H., Hamza, A.*, et al.*: 'Using general linear model, Bayesian networks and Naive Bayes classifier for prediction of *Karenia selliformis* occurrences and blooms', *Ecol. Inf.*, 2018, **43**, pp. 12–23